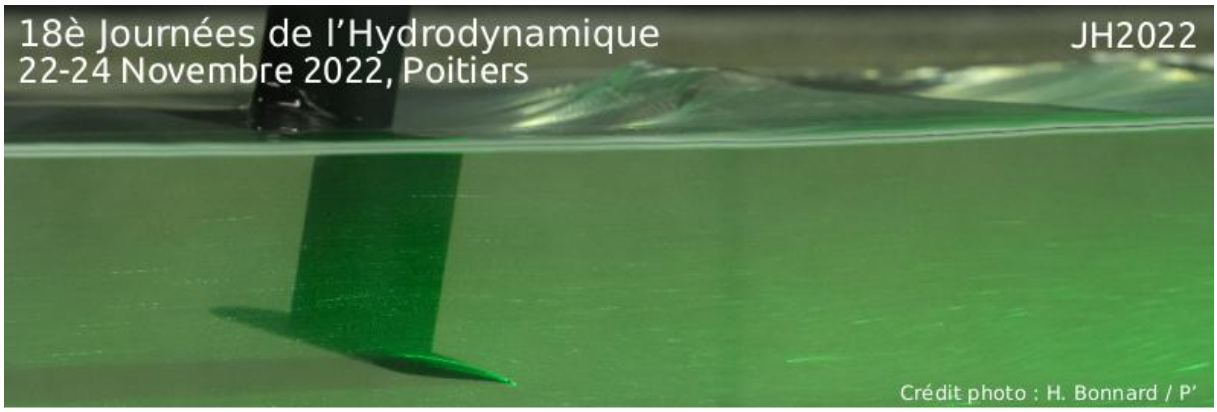

ÉVALUATION DE LA MÉTHODE MELNIKOV POUR LE PROBLÈME DU ROULIS DES NAVIRES

ASSESSMENT OF THE MELNIKOV METHOD FOR THE SHIP ROLL PROBLEM

CH. PAPOUTSELLIS[(1)], Y-M. SCOLAN[(1)]

christos.papoutsellis@ensta-bretagne.fr ; yves-marie.scolan@ensta-bretagne.fr

[(1)]Institut de Recherche Dupuy de Lôme, École Nationale Supérieure de Techniques Avancées Bretagne, Centre National de la Recherche Scientifique, UMR6027

Résumé

Dans ce travail, nous considérons le problème de stabilité d'un navire en roulis sur une houle régulière ou aléatoire. Le mouvement est modélisé comme un oscillateur non-linéaire à un seul degré de liberté et nous tenons compte de la mémoire hydrodynamique dans le cas aléatoire. Les coefficients de les équations correspondent à des données réelles. L'excitation des vagues est périodique ou donnée par un spectre de vagues océaniques. Nous comparons les critères de chavirement obtenus par la méthode asymptotique de Melnikov avec des simulations numériques du bassin de sécurité.

Summary

We consider the problem of capsize of a rolling ship in regular or random beam seas. We use a widespread model of the motion in which the roll angle is described by a nonlinear oscillator with linear and quadratic damping and harmonic or random wave excitation. In the latter case, we also take into account the hydrodynamic memory effect. The coefficients in the equation are obtained as high-order approximations of real ship data. We calculate numerically capsize criteria in terms of the forcing parameters using Melnikov's asymptotic method and compare with numerical simulations of safe basins for random realisations of the wave excitation obtained from an ocean wave spectrum.

I – Introduction

The current criteria that deal with the prevention of capsize of ships are based on the righting arm which expresses the distance between the lines along which the resultants of weight and buoyancy act as the ship inclines [11]. There exist a consensus that these criteria should be improved. The reason is that they only take into account the restoring capability of the ship in still water and ignore potentially important hydrodynamic effects such as the added mass and damping moment, the viscous damping and the forcing due to waves [21, 2, 7, 16]. A typical scenario that may lead to capsize is a ship rolling under the action of waves turned in beam seas. The roll angle in this case is usually modelled as a single-degree-of-freedom (SDOF) forced non-linear oscillator with damping. We also adopt this approach in the present work.

A classical perturbative method to derive criteria for the loss of integrity of such a system is the Melnikov method [18]. It is based on the assumption that the forced and damped oscillator can be written as a weak perturbation of a Hamiltonian system that possesses a homoclinic or heteroclinic orbits. It has been applied to the ship rolling problem under harmonic excitation in [5, 17, 20, 25] and under random excitation in [8, 19, 24, 22, 12], for instance. One of the difficulties in the latter case is that if the excitation contains a broad range of frequencies (e.g. from an ocean wave spectrum) the added mass and damping coefficients, being themselves frequency dependent, must be evaluated at a certain frequency which is not a priori known. This can be avoided by considering a Cummins-type integro-differential equation [4] that contains a convolution term accounting for the history-dependent roll-radiation moment. This term, known as the hydrodynamic memory, influences the probability of capsize and a universal strategy for replacing it with constant added mass and damping coefficients does not seem plausible [9].

Another method, primarily developed for the harmonic excitation case, is to study the safe basin of the system by solving it numerically for several initial conditions and characterise each of them as safe or unsafe [23, 25, 14]. Significant changes in the shape and form of the safe basin (erosion) are associated with loss of structural integrity of the system under study. This approach does not require a smallness assumption on the perturbation but is characterised by an increased computational cost especially when the hydrodynamic memory is taken into account. We extend this approach to the case of a random wave excitation given by an ocean wave spectrum and use these results to assess the critical parameters obtained by the Melnikov method.

II – The modelling of ship rolling

The roll angle with respect to the calm sea surface at time τ is denoted by $\phi(\tau)$ and is considered uncoupled from the other ship motions. In the case of a harmonic forcing of frequency ω, $\phi(\tau)$ satisfies

$$(I_{44} + A_{44}(\omega))\frac{\mathrm{d}^2\phi}{\mathrm{d}^2\tau} + (B_{44}(\omega) + B_1)\frac{\mathrm{d}\phi}{\mathrm{d}\tau} + B_2\frac{\mathrm{d}\phi}{\mathrm{d}\tau}\left|\frac{\mathrm{d}\phi}{\mathrm{d}\tau}\right| + \Delta\, P(\phi) = F_{44}(\omega)A\cos(\omega\tau) \quad (1)$$

where I_{44} is the rotational moment of inertia of the dry vessel about the rolling axis, $A_{44}(\omega)$ is the added mass moment and $B_{44}(\omega)$ is the added damping coefficient. The coefficients B_1 and B_2 are viscous linear and quadratic roll damping coefficients respectively. The term $\Delta\, P(\phi)$ represents the restoring moment experienced by the vessel in still water as a function of ϕ and is obtained as the product of the vessel displacement Δ with a highly

non-linear odd polynomial $P(\phi)$ that vanishes at $\phi = 0$ and at the *angle of vanishing stability*, $\phi = \phi_v$. $P(\phi)$ approximates the graph of righting arm $GZ(\phi)$. The right hand side (rhs) of (1) is the wave-induced moment excitation about the roll axis obtained as the product of the sinusoidal free-surface elevation of amplitude A and frequency ω (wave height $H = 2A$) with the roll moment per unit wave amplitude $F_{44}(\omega)$.

In the random forcing case, the ship-roll equation takes the substantially different form of a Volterra Integro-Differential Equation (IDE) [9] :

$$(I_{44} + A_{44}(\infty))\,\frac{\mathrm{d}^2\phi}{\mathrm{d}\tau^2} + (B_{44}(\infty) + B_1)\,\frac{\mathrm{d}\phi}{\mathrm{d}\tau} + B_2\frac{\mathrm{d}\phi}{\mathrm{d}\tau}\left|\frac{\mathrm{d}\phi}{\mathrm{d}\tau}\right| + \\ + \int_0^\tau K(\tau-\sigma)\frac{\mathrm{d}\phi}{\mathrm{d}\tau}(\sigma)\,\mathrm{d}\sigma + \Delta P(\phi) = F(\tau), \quad (2)$$

where $K(\tau)$ is the hydrodynamic rolling moment due to impulse roll velocity also known as the impulse response function (IRF) [4, 15, 10] or the hydrodynamic memory function because it represents how roll-radiation moments depend on the history of the rolling velocity. In Eq. (2), the forcing $F(\tau)$ is a random process. If the free-surface elevation $\eta(\tau)$ is a stationary ergodic Gaussian stochastic process with a spectrum $S_\eta(\omega)$, then the spectrum of $F(\tau)$ is given by

$$S_F(\omega) = F_{44}(\omega)^2 S_\eta(\omega). \quad (3)$$

Here, we use the Modified Pierson-Moskowitz (MPM) Spectrum which is considered appropriate for the response of marine vehicles and offshore structures in fully developed infinite-depth wind-generated seas with no swell and unlimited fetch [6].

The quantities described above are obtained by linear hydrodynamic calculations or experiments and are available for discrete values of ω or ϕ. For the purposes of Eqs. (1) and (2) a suitable processing of these data is required. The righting arm is approximated by a 9^{th} degree odd polynomial. The added damping coefficient is interpolated up to the frequency available by the hydrodynamic calculations and then it is extrapolated exponentially. This is required for the calculation of the IRF function [1]. A typical example is shown in figure 1.

III – The Melnikov method

In order to apply the Melnikov method, Eqs. (1) and (2) must be written as weakly perturbed Hamiltonian systems. This is done by using the scalings

$$t = \omega_n\tau, \quad \omega_n^2 = \frac{C_1\Delta}{I_{44} + A_{44}(\omega_n)}, \quad \text{and} \quad t = \omega_\nu\tau, \quad \omega_\nu^2 = \frac{C_1\Delta}{I_{44} + A_{44}(\infty)}, \quad (4)$$

in Eq. (1) and (2) respectively. For Eq. (1), we obtain

$$\begin{aligned} \dot{x} &= y \\ \dot{y} &= -p(x) - \epsilon\left(\beta_1 y + \beta_2 y|y| + \alpha\cos(\Omega t)\right) \end{aligned} \quad (5)$$

where $x(t) = \phi(\tau)$, $\Omega = \omega/\omega_n$,

$$p(x) = x + \frac{C_3}{C_1}x^3 + \frac{C_5}{C_1}x^5 + \ldots \quad (6)$$

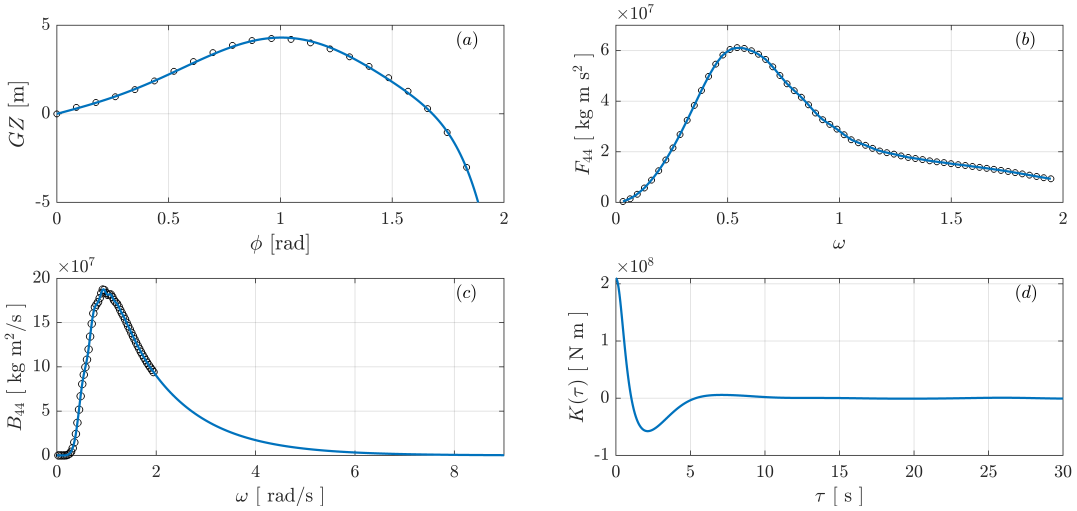

FIGURE 1 – (a) GZ-curve and interpolating polynomial $P(\phi)$ of 9^{th} degree, (b) added damping coefficient $B_{44}(\omega)$ obtained via interpolation and exponential extrapolation, (c) Calculated impulse response function $K(\tau)$, (d) Roll moment per unit wave amplitude $F_{44}(\omega)$ and interpolating curve. The hydrodynamic data are shown with circles and correspond to a real ship hull.

and

$$\epsilon\beta_1 = \frac{B_{44}(\omega) + B_1}{C_1\Delta}\omega_n, \quad \epsilon\beta_2 = \frac{B_2}{C_1\Delta}\omega_n^2, \quad \epsilon\alpha = \frac{AF_{44}(\omega)}{C_1\Delta}, \tag{7}$$

Similarly, for Eq. (2) we have

$$\begin{aligned} \dot{x} &= y \\ \dot{y} &= -p(x) - \epsilon\left(\beta_1 y + \beta_2 y|y| + \int_0^t k(t-s)y(s)\,\mathrm{d}s\right) + \epsilon f(t) \end{aligned} \tag{8}$$

where

$$\epsilon\beta_1 = \frac{B_1}{C_1\Delta}\omega_\nu, \quad \epsilon\beta_2 = \frac{B_2}{C_1\Delta}\omega_\nu^2, \quad \epsilon k(t) = \frac{K(t)\omega_\nu^2}{C_1\Delta}, \quad \epsilon f(t) = \frac{F(t/\omega_\nu)}{C_1\Delta}. \tag{9}$$

III – 1 The unperturbed system

The unperturbed system obtained from (5) or (8) with $\epsilon = 0$ is an integrable Hamiltonian system with potential energy of the typical form of a single well shown in figure 2(a). It possesses three fixed points, one stable center $O(0,0)$ and two saddle equilibrium points $O_+(\phi_v, 0)$ and $O_-(-\phi_v, 0)$ which are connected by a symmetric pair of heteroclinic orbits denoted by $\mathbf{x}_h^+(t) = (x_h(t), y_h(t))$ and $\mathbf{x}_h^-(t) = (-x_h(t), -y_h(t)) = -\mathbf{x}_h^+(t)$, see figure 2(b). These orbits define the coincident stable and unstable manifolds of the two saddles $O_+(\phi_v, 0)$ and $O_-(-\phi_v, 0)$ and separate the phase space into two qualitatively distinct regions ; a bounded region, known as the *safe basin*, and its complement. Any motion that starts from within the safe basin remains bounded, whereas any motion that starts from its complement becomes unbounded.

III – 2 The Melnikov function

In the presence of a small perturbation, $0 < \epsilon \ll 1$, the perturbed stable and unstable manifolds do not coincide anymore. Their signed distance is measured in terms of the

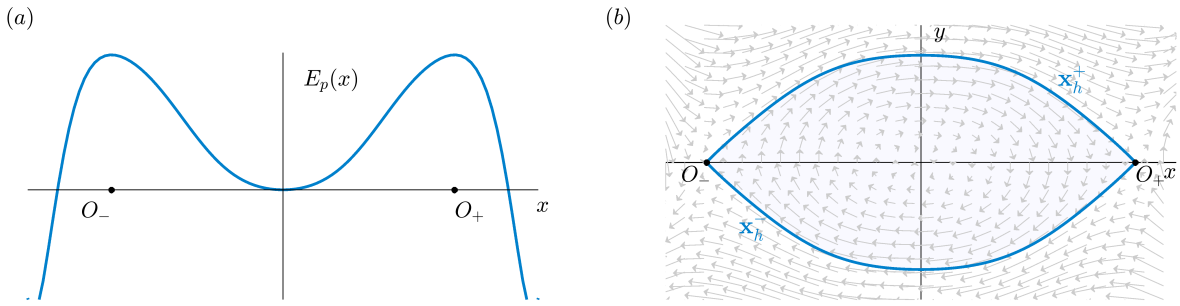

FIGURE 2 – (a) Potential well (b) Heteroclinic cycle $\mathbf{x}_h^+ \cup \mathbf{x}_h^- \cup O_+ \cup O_-$ and vector field $\mathbf{f}$ of the unperturbed system

position of the unperturbed manifolds. The first order approximation of this distance is the Melnikov function. For a perturbed Hamiltonian system of the form

$$\dot{\mathbf{x}} = \mathbf{f}(\mathbf{x}) + \epsilon \mathbf{g}(\mathbf{x}, t), \quad \mathbf{f}(\mathbf{x}) = \begin{pmatrix} y \\ -p(x) \end{pmatrix}, \tag{10}$$

with $\mathbf{x} = (x, y)$, and $\mathbf{g} = (0, g(\dot{x}))^{\mathrm{T}}$, the Melnikov function $M(t_0)$ is given by

$$M(t_0) = -\int_{-\infty}^{\infty} \dot{x}_h(s) g(\dot{x}_h)\, \mathrm{d}s + \int_{-\infty}^{\infty} \dot{x}_h(s) f(s + t_0)\, \mathrm{d}s = \overline{M} + \widetilde{M}(t_0), \tag{11}$$

and is composed by a constant and a time-dependent part as also suggested by the introduced notation [18]. If $M(t_0) > 0$, then the perturbed stable and unstable manifolds intersect transversely which means that safe points of the phase-space may now be found in the exterior of the safe basin. This fact is used for the determination of critical parameters for which this condition is satisfied. The evaluation of $M(t_0)$ requires the calculation of the heteroclinic orbit of the unperturbed system which is performed numerically.

III – 2.1 Harmonic wave forcing

In the case of system (5), $g(y) = -\beta_1 y - \beta_2 y|y| + \alpha \cos(\Omega t)$, and we have

$$\overline{M} = \beta_1 \int_{-\infty}^{\infty} y_h^2 \mathrm{d}t + \beta_2 \int_{-\infty}^{\infty} y_h^2 |y_h| \mathrm{d}t \tag{12}$$

$$\widetilde{M}(t_0) = \alpha \int_{-\infty}^{\infty} y_h(s) \cos\left[\Omega(s + t_0)\right] \mathrm{d}s = \alpha C(\Omega) \cos(\Omega t_0) \tag{13}$$

where

$$C(\Omega) = \int_{-\infty}^{\infty} y_h(s) \cos(\Omega s) \mathrm{d}s,$$

see e.g. [3], [18, Sec. 2.5.3]. $M(t_0)$ has a simple zero at some t_0 if and only if $\alpha C(\Omega) > \overline{M}$. Thus, taking the equality, we may define a critical forcing amplitude beyond which transverse intersection of the stable and unstable manifold occurs for a given Ω. The corresponding critical wave height is given by

$$H^*(\Omega) = 2C_1 \Delta \frac{|\epsilon \overline{M}|}{F_{44}(\Omega \omega_n) C(\Omega)}. \tag{14}$$

III – 2.2 Random wave forcing

In the case of system (8), we have [9]

$$\overline{M} = \beta_1 \int_{-\infty}^{\infty} y_h^2 \, \mathrm{d}t + \beta_2 \int_{-\infty}^{\infty} y_h^2 |y_h| \, \mathrm{d}t + \int_{-\infty}^{\infty} y_h(t) \int_{-\infty}^{+\infty} k(t-s) y_h(s) \, \mathrm{d}s \, \mathrm{d}t \tag{15}$$

$$\widetilde{M}(t_0) = \int_{-\infty}^{\infty} y_h(s) f(s+t_0) \, \mathrm{d}s \, . \tag{16}$$

Here, $\widetilde{M}(t_0)$ is a random process defined by a linear transformation of the Gaussian process $f(t)$, hence it is also a Gaussian process. Its root expected value is $E[\widetilde{M}(t_0)] = 0$, provided that $E[f(t)] = 0$. Its mean square value depends on the random wave excitation parameters parameters (significant wave height H_s and characteristic frequency ω_z) and is given by

$$\sigma(\Omega, H_s) = E[\widetilde{M}(t_0)^2] = \int_0^{+\infty} 2\pi \, S_{y_h}(\Omega) \, S_f(\Omega) \, \mathrm{d}\Omega \tag{17}$$

where $\Omega = \omega_z/\omega_\nu$, $S_{y_h}(\Omega)$ is the spectrum of the heteroclinic orbit and $S_f(\Omega)$ is the spectrum the forcing [8, 9] . Since the probability of $M(t_0)$ having simple zeros is non-zero, a critical wave height in this case is obtained in terms of the phase-space transport. Phase-space transport occurs as regions of the phase space are transported out of the safe basin when the stable and unstable manifolds intersect. The sum of the areas of these regions can be approximated at first order in ε in terms of $\widetilde{M}(t_0)$ and the rate of phase-space flux can be estimated. We refer to [18, 8, 9] for the details. The critical wave height in this approach is defined in terms of the theoretical asymptote of the phase-space flux as a function of the wave-height and is given by

$$H_s^*(\Omega) = \frac{\sqrt{2\pi}\, \epsilon \overline{M}}{2\sigma(\Omega, 1)}, \tag{18}$$

This H_s^* gives a threshold after which substantial phase-space flux begins to occur, at first order in ϵ.

IV – The concept of the erosion of the safe basin

In this approach, the capsize is identified as the escape from a potential well [23]. For any given set of initial conditions and excitation function, it is possible to solve numerically (5) and (8) for a certain amount of time and judge if the ship has capsized or not based on if the roll angle has exceeded the angle of vanishing stability. The subset of initial conditions that did not lead to capsize after some specified duration D designates the safe basin of our perturbed system. For the system (5) we use a classical 4^{th}-order Runge-Kutta method while for the integro-differential Eq. (8) we implemented a 4^{th}-order Runge-Kutta method of Bel'tyukov type [13] in order to accurately take into account the convolution term. We generate approximate realisations of the random process $F(t)$ as superpositions of trigonometric functions with random phase. The mean integrity of the safe basin is measured using the index

$$\mathcal{I} = \frac{1}{N} \sum_{n=1}^{N} \frac{\text{Area}(S_n)}{\text{Area}(S_{\text{uf}})} \tag{19}$$

where N is the number of realisations, S_n is the safe basin corresponding to the n^{th} realisation and S_{uf} is the safe basin of the unforced system, that is Eqs. (5) or (8) without forcing. Obviously, in the deterministic case $N = 1$.

V – Results

In this section, we compare the critical curves obtained by the deterministic and stochastic Melnikov method with the results obtained by numerical simulations of the safe basins. For the harmonic excitation case the simulation time is $D = 15(2\pi/\omega)$ s where $\omega = \Omega\omega_n$ is the forcing frequency. In this case, the linear damping coefficient $\varepsilon\beta_1$ ranges from 0.015 to 0.04. In the random excitation case we have used $\varepsilon\beta_1 = 0.015$, $D = 900$ s and $N = 150$ realisations of the MPM spectrum. The phase space is discretised in 150^2 cells covering all possible initial positions and velocities. We also consider three values of the quadratic damping coefficient $\varepsilon\beta_2$ in order to study its effect. We plot the results on the safe-basin integrity $\mathcal{I}$ as a function of the forcing frequency parameters together with the Melnikov curves (14) and (18) in figure 3.

In both cases, the Melnikov curves are in qualitative agreement with the contour lines of $\mathcal{I}$ corresponding to the percentage of the unforced safe basin that survived at the end of the simulations. In the harmonic excitation case, severe erosion occurs in a small localised region around the natural frequency. Also, the erosion becomes more abrupt as it can be inferred by the converging contour lines. The Melnikov curves, give a rather conservative prediction of the onset of erosion when $\varepsilon\beta_2$ is weak and become less conservative with increasing $\varepsilon\beta_2$. A similar effect is also reported in [25] in terms of the linear damping.

In the case of a broad band random excitation, severe erosion occurs for a wider range of frequencies and this is qualitatively captured by the Melnikov curve defined by (18). As $\varepsilon\beta_2$ increases, the Melnikov curve clearly enters in the unsafe region where a significant probability of capsize is expected. We mention, for example, that along the Melnikov curves the probability of capsize after time D of a ship initially at rest in a up-right position is 0% for $\varepsilon\beta_2 = 0.005$ and ranges from 3% to 40% for $\varepsilon\beta_2 = 0.05$ and from 70% to 100% for $\varepsilon\beta_2 = 0.10$. This is because (18) gives a rough asymptotic estimation on the critical wave height which is not applicable for large $\varepsilon\beta_2$. An option would be to modify the definition of critical wave height in terms of a percentage of the phase space flux [19].

VI – Conclusions and perspectives

We have implemented the Melnikov method for the SDOF ship-roll escape equation with a single-well potential of degree 9, linear and quadratic damping and harmonic or Gaussian excitation given by an ocean wave spectrum. In the latter case, we also take into account the hydrodynamic memory via the convolution term in the Cummins equation. In order to gain confidence on the critical wave height obtained by the Melnikov method we have compared our results with highly accurate calculations of the safe basins for a broad range of the forcing parameters (frequency and wave height). In the harmonic excitation case, the Melnikov curves are below the onset of basin erosion and become less conservative as the quadratic damping increases. A similar situation occurs in the random excitation case. In fact, the critical wave height seems inadequate for large quadratic damping.

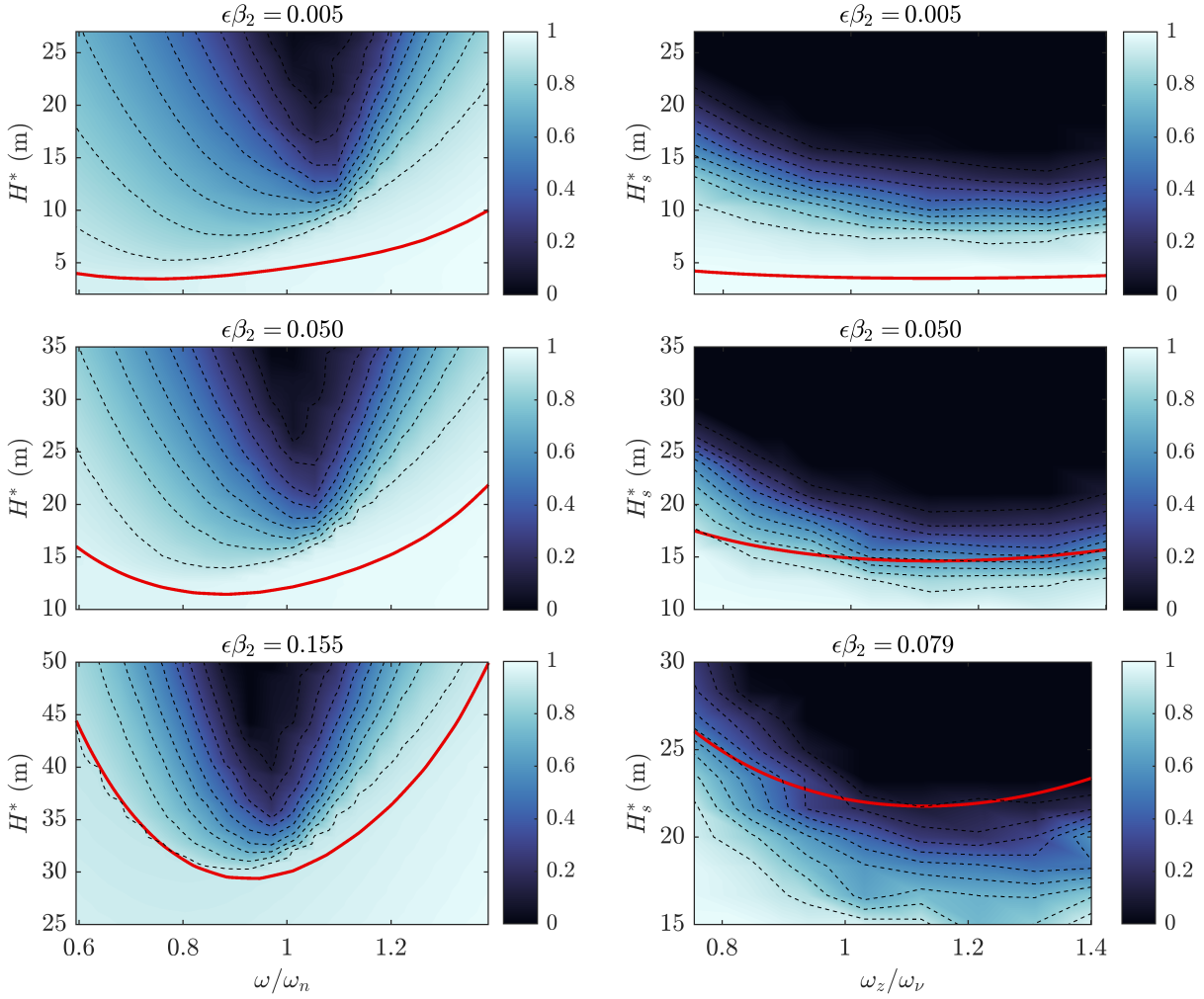

FIGURE 3 – Integrity $\mathcal{I}$ of the safe basin for different values of the quadratic damping coefficient $\varepsilon\beta_2$ for the harmonic excitation case (left) and the random excitation case (right). Solid red lines correspond to the Melnikov curves. Dashed lines are contour lines representing the percentage of the unforced safe basin left at the end of the simulation starting from 0.9 and decreasing by 0.1.

Acknowledgements

This work was carried out in the framework of the STADYNAV project funded by the "Agence de l'Innovation de Défense" of the "Direction Générale de l'Armement".

Références

[1] J. Armesto, R. Guanche, and F. J. et al. Comparative analysis of the methods to compute the radiation term in Cummins' equation. *J. Ocean Eng. Mar. Energy*, 1 :377–393, 2015.

[2] L. Arnold, I. Chueshov, and G. Ochs. Stability and capsizing of ships in random sea - a survey. *Nonlinear Dyn.*, 36 :135–179, 2004.

[3] M. Bikdash, B. Balachandran, and A. Navfeh. Melnikov analysis for a ship with a general roll-damping model. *Nonlinear. Dyn.*, 6 :101–124, 1994.

[4] W. Cummins. The Impulse Response Function and Ship Motions. *Navy Department, David Taylor Model Basin*, 1962.

[5] J. M. Falzarano, S. W. Shaw, and A. W. Troesch. Application of global methods for analyzing dynamical systems to ship rolling motion and capsizing. *International Journal of Bifurcation and Chaos*, 02(01) :101–115, 1992.

[6] T. Fossen. *Guidance and control of ocean vehicles*. John Wiley and sons, Chichester, England, 1988.

[7] A. Francescutto. Intact stability criteria of ships – past, present and future. *Ocean Engineering*, 120 :312–317, 2016.

[8] S. Hsieh, A. W. Troesch, and S. Shwa. A nonlinear probabilistic method for predicting vessel capsizing in random beam seas. *Philos. Trans. R. Soc. A*, 446 :195–211, 1994.

[9] C. Jiang, A. W. Troesch, and S. W. Shaw. Capsize criteria for ship models with memory-dependent hydrodynamics and random excitation. *Philos. Trans. R. Soc. A*, 358(1771) :1761–1791, 2000.

[10] M. Kashiwagi. Transient responses of a VLFS during landing and take-off of an airplane. *J. Mar. Sci. Technol.*, 9 :14–23, 2004.

[11] E. V. Lewis. *Principles of Naval Architecture Second Revision*, volume 1. The Society of Naval Architects and Marine Engineers, 1988.

[12] Y. Li, Z. Wei, T. Kapitaniak, and W. Zhang. Stochastic bifurcation and chaos analysis for a class of ships rolling motion under non-smooth perturbation and random excitation. *Ocean Eng.*, 266 :112859, 2022.

[13] C. Lubich. Runge-Kutta theory for Volterra integrodifferential equations. *Numerical Mathematics*, 40 :119–135, 1982.

[14] A. Maki, Y. Miino, N. Umeda, M. Sakai, T. Ueta, and H. Kawakami. Nonlinear dynamics of ship capsizing at sea. *Nonlinear Theory and Its Applications, IEICE*, 13(1) :2–24, 2022.

[15] T. F. Ogilvie. Recent progress toward the understanding and prediction of ship motions. In *Proceedings of the 5th Symposium on Naval Hydrodynamics*, pages 3–80, Bergen, Norway, 1964. 5th Symp. On Naval Hydrodynamics.

[16] N. Petacco and P. Gualeni. Imo second generation intact stability criteria : General overview and focus on operational measures. *J. mar. sci*, 8(7), 2020.

[17] Y. Scolan. Technical note on ship rolling associated to high degree polynomial restoring moment using the melnikov method. *Appl. Ocean Res.*, 19(3) :225–234, 1997.

[18] E. Simiu. *Chaotic Transitions in Deterministic and Stochastic Dynamical Systems : Applications of Melnikov Processes in Engineering, Physics, and Neuroscience*. Princeton University Press, Princeton, 2002.

[19] A. Somayajula and J. Falzarano. Parametric roll vulnerability of ships using Markov and Melnikov approaches. *Nonlinear Dyn.*, 97(17) :1977–2001, 2019.

[20] K. Spyrou, B. Cotton, and B. Gurd. Analytical Expressions of Capsize Boundary for a Ship with Roll Bias in Beam Waves. *J. Ship Res.*, 46(03) :167–174, 09 2002.

[21] K. Spyrou and J. Thompson. The nonlinear dynamics of ship motions : a field overview and some recent developments. *Phil. Trans. R. Soc. Lond. A*, 358(1771) :1735–1760, 2000.

[22] Z. Su and J. M. Falzarano. Markov and Melnikov based methods for vessel capsizing criteria. *Ocean Eng.*, 64 :146–152, 2013.

[23] J. M. T. Thompson, R. C. T. Rainey, and Soliman. Ship stability criteria based on chaotic transients from incursive fractals. *Philos. Trans. Royal Soc. A*, 332(1624) :149–167, 1990.

[24] S. Vishnubhotla, J. Falzarano, and A. Vakakis. A new method to predict vessel/platform critical dynamics in a realistic seaway. *Philos. Trans. A Math. Phys. Eng.*, 358(1771) :1967–1981, 2000.

[25] W. Wu and L. McCue. Application of the extended melnikov's method for single-degree-of-freedom vessel roll motion. *Ocean Eng.*, 35(17) :1739–1746, 2008.